ACS chemical biology

ARTICLES

pubs.acs.org/acschemicalbiology

Elucidation of the Hsp90 C-Terminal Inhibitor Binding Site

Robert L. Matts,[†] Anshuman Dixit,[‡] Laura B. Peterson,[§] Liang Sun,[†] Sudhakar Voruganti,[†] Palgunan Kalyanaraman,[†] Steve D. Hartson,[†] Gennady M. Verkhivker,[⊥] and Brian S. J. Blagg[§,*]

[†]Department of Biochemistry and Molecular Biology, NRC 246, Oklahoma State University, Stillwater, Oklahoma 74078, United States

[‡]The Center for Bioinformatics, The University of Kansas, 2030 Becker Drive, Lawrence, Kansas 66045, United States

[§]Department of Medicinal Chemistry, The University of Kansas, 1251 Wescoe Hall Drive, 4070 Malott, Lawrence, Kansas 66045-7582, United States

[⊥]Department of Pharmacology, University of California, San Diego, 9500 Gilman Dr., La Jolla, California 92093-0636, United States

Supporting Information

ABSTRACT: The Hsp90 chaperone machine is required for the folding, activation, and/or stabilization of more than 50 proteins directly related to malignant progression. Hsp90 contains small molecule binding sites at both its N- and C-terminal domains; however, limited structural and biochemical data regarding the C-terminal binding site is available. In this report, the small molecule binding site in the Hsp90 C-terminal domain was revealed by protease fingerprinting and photoaffinity labeling utilizing LC−MS/MS. The identified site was characterized by generation of a homology model for hHsp90α using the SAXS open structure of HtpG and docking the bioactive conformation of NB into the generated model. The resulting model for the bioactive conformation of NB bound to Hsp90α is presented herein.

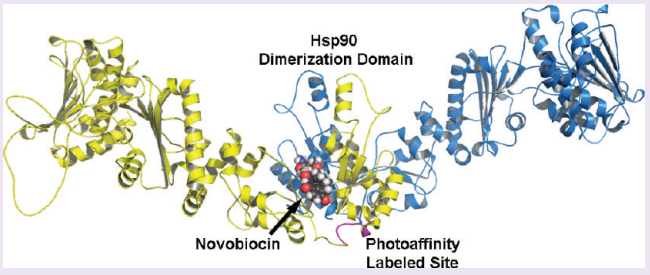

Hsp90 is the core component of a chaperone machine that modulates the folding, activation, and stability of more than 200 substrates. Hsp90 functions by undergoing a series of conformational changes that are driven by the binding and hydrolysis of ATP, which are modulated through Hsp90's interactions with a variety of co-chaperones and partner proteins (reviewed in refs 1 and 2). Because Hsp90-dependent clients are directly associated with all six hallmarks of cancer,[3] Hsp90 is under intense investigation as a pharmacological target for the treatment of cancer.[4,5]

Hsp90 contains drugable sites at both its N- and C-terminal domains. High affinity Hsp90 inhibitors that bind the Hsp90 N-terminal nucleotide binding site are well characterized, as they have been co-crystallized with this domain (*i.e.*, geldanamycin and radicicol[6,7]). In fact, several N-terminal inhibitors are currently in clinical trials for the treatment of cancer.[8] In 2000, Neckers and co-workers identified the first C-terminal inhibitor of Hsp90[9,10] by demonstrating the ability of the Hsp90 C-terminus to bind novobiocin (NB) (Figure 1) and proposed this domain to represent a nucleotide-binding site that allosterically regulates nucleotide binding at the N-terminus.

Not only does NB inhibit Hsp90 function by binding to the C-terminus of Hsp90, but related family members chlorobiocin (CB) and coumermycin A1 also display Hsp90 inhibitory profiles that are different from those manifested by N-terminal inhibitors (Figure 1). In addition, C-terminal inhibitors exhibit unique effects on Hsp90's conformation, activity, and interactions with co-chaperones and clients,[9−12] highlighting this site as a potential target for Hsp90 modulation. Unfortunately, the mechanism of action for Hsp90 "C-terminal inhibitors" has not been adequately pursued, in large part due to their poor pharmacological potencies (100−700 μM).[9,10,12,13] Although analogues of NB that exhibit improved Hsp90-inhibitory and anticancer activity[14−19] have been reported, the inability to obtain co-crystal structures with these molecules bound to the chaperone has hampered further development.

Crystal structures of yeast Hsp90, its human ER homologue (Grp94), and *E. coli* homologue (HtpG) have provided insights into the conformational changes Hsp90 undergoes during the substrate folding process. In addition, low resolution small-angle X-ray scattering (SAXS)[20,21] and cryo-electron microscopy studies[22,23] have provided additional evidence in support of the multiple conformations necessary for folding client substrates. While SAXS[20,21] and cryo-electron microscopy[22,23] studies have clearly demonstrated the Hsp90 C-terminus to adopt distinct conformations, these structures have not provided the resolution necessary for structure-based drug design of improved inhibitors. Unfortunately, the available structures of Hsp90's C-terminal domain and its homologues are similar and represent the closed, clamped conformation, in which the apparent binding site is

Received: November 9, 2010
Accepted: May 6, 2011
Published: May 06, 2011

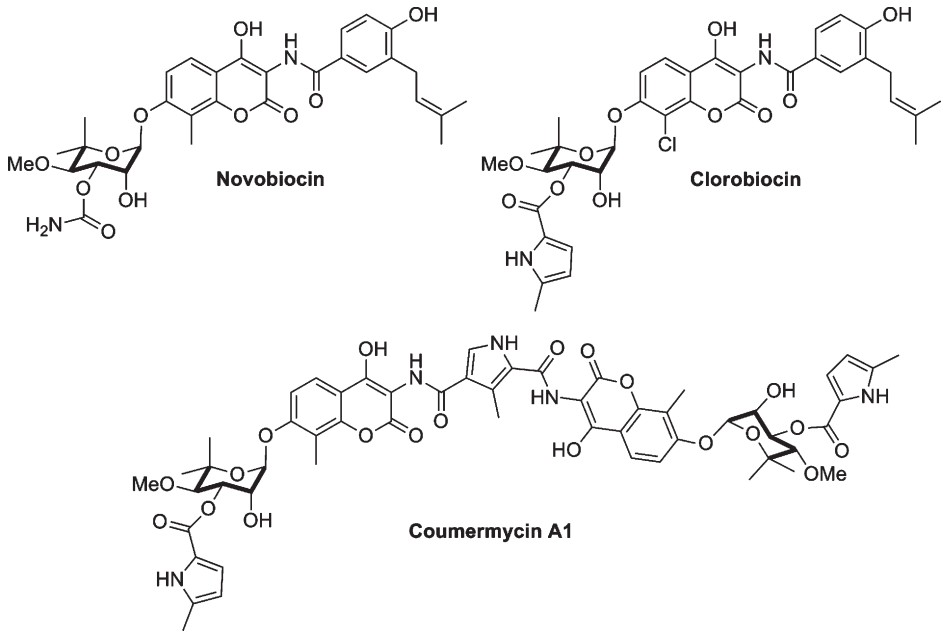

Figure 1. Representative Hsp90 C-terminal inhibitors.

inaccessible. In addition, as first suggested by Agard and co-workers, Hugel and co-workers have recently confirmed that the Hsp90 C-terminus undergoes significant conformational changes and opens across the dimerization domain upon occupation of the N-terminal ATP binding site providing a potential mechanism for client protein release.[24]

To circumvent limitations imposed upon the rational development of NB analogues through a structure-based approach, the NB binding site located in the Hsp90 C-terminus was sought after *via* photolabile NB derivatives, which upon covalent attachment to Hsp90 could aid in elucidation of the Hsp90 C-terminal binding site. Subsequent refinement of the biologically active conformation of NB bound to Hsp90 could then be derived from the SAXS structure of HtpG in its open conformation, which allows occupancy of the C-terminus. As revealed by co-crystal structures of NB bound to closely related enzymes (*e.g.*, DNA gyrase/topoisomerase[25,26]), the active conformation of NB could then be docked and subjected to a ligand-supported refinement, followed by a systematic molecular dynamics (MD) based methodology to outline the binding site for NB. Herein, we present our approach toward elucidation of the Hsp90 C-terminal binding site following this protocol.

RESULTS AND DISCUSSION

Identification of the Hsp90 C-Terminal Protease-Resistant Core. Binding of NB and chlorobiocin (CB) to the Hsp90 C-terminus protects this domain from proteolysis by trypsin,[12] which is not the case for N-terminal inhibitors, suggesting that C-terminal occupancy plays a significant role in protein conformation. Surface plasmon resonance spectroscopy analysis of the binding of chlorobiocin and coumerimycin A1 to full length Hsp90 and Hsp90CT indicates that the C-terminal domain of Hsp90 binds the compounds with affinities comparable to that of the intact, full length protein, suggesting truncation does not compromise the structure of the Hsp90's C-terminal binding site (R. L. Matts, J. R. Manjarrez, and K. Szalba, unpublished results).

To determine the amino acid residues that define the CB-bound protease-resistant core of Hsp90, a His-tagged Hsp90 C-terminal construct was digested with V8 protease in the presence and absence of chlorobiocin. V8 was chosen because the N- and C-terminal regions of Hsp90 are deficient in Lys and Arg residues but rich in Glu and Asp.

Upon SDS-PAGE analysis of Hsp90 C-terminal proteolysis products, four bands were found resistant to V8 cleavage in samples containing CB that were absent from the control (Figure 2A). Analysis of the in-gel tryptic digests of each band by nanospray-MS/MS is summarized in Figure 2. Band a was generated in both the control and CB-treated samples on ice upon treatment with V8 protease, which corresponds to cleavage at the first Glu residue in the N-terminus of the Hsp90CT construct, which removes the His-tag (Figure 2 and Supplemental Figure 1). The tryptic peptides identified in each band are described in Figure 2B. Band c contained the tryptic peptide spanning residues Glu547−Lys588 but lacked the tryptic/V8 peptides corresponding to the Leu694−Glu714/Glu715 peptides present in bands d and e. Band c also lacked the tryptic peptide Leu694-Arg727 generated from the C-terminal end of band b, suggesting that band c had a V8 cut between residue Glu714 and Arg727. Regardless of the exact position of the C-terminal V8 cleavage of band c, the analysis of the two lower MW bands (d/e) localizes the CB-bound protease-resistant core of Hsp90CT to residues Gly548-Glu714 (Figure 2), which is consistent with Neckers prior studies that identified residues 538−728. Overall, the data suggest that the binding of chlorobiocin to the Hsp90CT is within a region that connects the middle domain of Hsp90 to its C-terminal domain and protects this region from proteolysis as highlighted in yellow and red in Figure 2D, corresponding to each monomer of the Hsp90 homodimer.

Identification of the NB Binding Site in Hsp90's C-Terminal Domain. Photolabile derivatives of novobiocin were synthesized for the purpose of identifying the Hsp90 C-terminal binding site.[27] As noted earlier, the Hsp90 C-terminus is resistant to proteolysis by trypsin in the presence of chlorobiocin. Similarly,

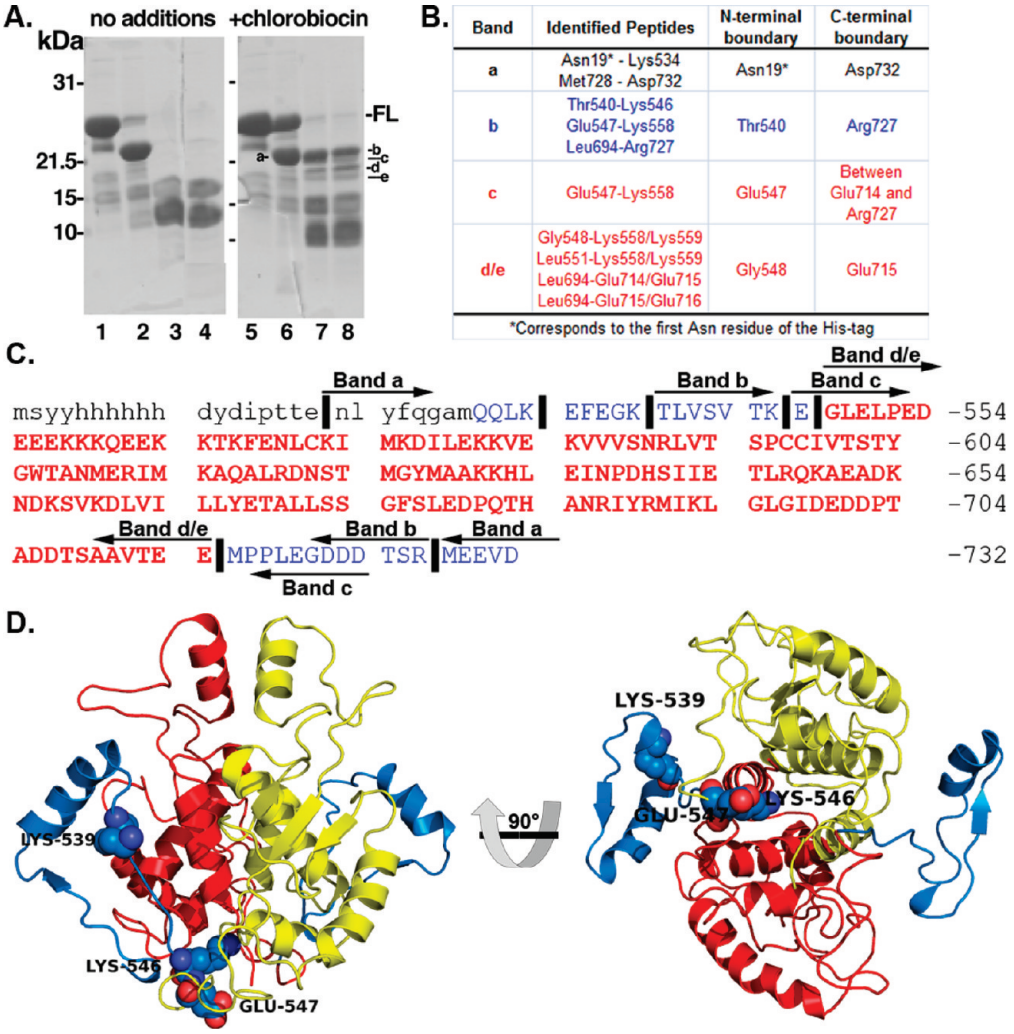

Figure 2. V8 protease-resistant core of Hsp90's C-terminal domain. (A) Protease resistance of chlorobiocin-bound Hsp90CT. Hsp90CT was incubated in the presence (lanes 2−4 and 6−8) of V8 protease with the addition of DMSO (vehicle control: lanes 1−4) or 800 mM chlorobiocin (lanes 5−8) for 0 min (lanes 2 and 6), 15 min (lanes 3 and 7), or 30 min (lanes 4 and 8). Lanes 1 and 5: Undigested full length Hsp90CT (-FL). Protease-resistant bands a−e as indicated. (B) Table including the sequences identified and boundaries for each band identified after proteolysis and SDS-PAGE. Red and blue rows correspond to the protease-resistant core and flanking regions, respectively. (C) Sequence of the Hsp90 C-terminus. Lower and upper case letters indicate residues from the His-tag and Hsp90 C-terminus, respectively. Vertical lines (|) indicate important cleavage sites that define the boundaries of bands a−e. Peptide bands a−e are depicted by left and right arrows denoting N- and C- termini of these bands. Bold and red residues comprise the chlorobiocin-induced Hsp90 CT protease-resistant core. (D) Hsp90 C-terminus, important cleavage sites labeled (spheres); red and yellow cartoons provide the protease-resistant core from each Hsp90 monomer, while blue cartoon indicates residues not part of the protease-resistant core.

compound **1a** also protected the Hsp90 C-terminus from trypsin proteolysis (Figure 3), indicating that the photolabile compound bound Hsp90 in a manner similar to that of novobiocin and chlorobiocin[12] (see Supplemental Figure 1C).

Novobiocin analogues containing a photoreactive azide moiety placed in the *p*- (**1a**/**1b**) or *m*-position (**2**) were used in lieu of the phenol and prenyl side chain present in NB, respectively. A recombinant His-tagged Hsp90 C-terminal construct was incubated in the presence or absence of **1a**[27] followed by UV irradiation. No change in the m/z of Hsp90CT was detected upon MALDI-TOF analysis of the Hsp90 C-terminus upon UV irradiation in the absence of **1a** (Figure 4A); however, in the presence of **1a** a new polypeptide peak (m/z = 25,125) with a mass approximately 545 Da greater than the parental peak (m/z = 24,580) was detected (Figure 4B), which corresponds to the molecular weight of compound **1a** minus one molecule of N_2.

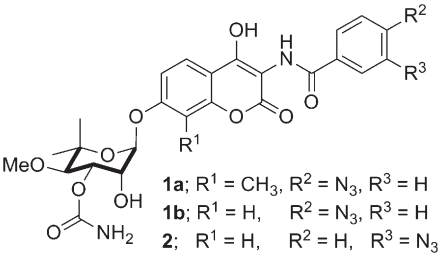

Figure 3. Novobiocin derivatives used in photoaffinity labeling studies.

To confirm that both the azide-containing molecule and the nonlabeled novobiocin bind to the same location, cross-linking studies were carried out in the presence of an equimolar concentration of NB and **1a**, resulting in a >80% decrease in the intensity

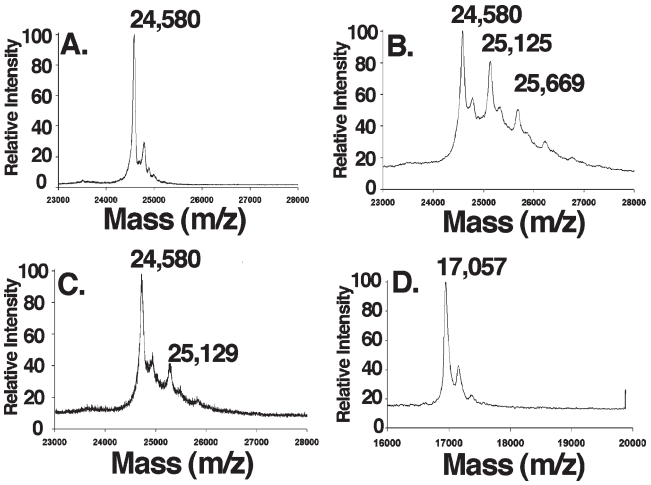

Figure 4. Cross-linking of **1** to Hsp90CT is specific. Hsp90CT (a−c) or apomyogobin (d) were UV irradiated as described in Methods in the presence of (A) DMSO, (B, D) 5 mM **1a**, or (C) 5 mM **1a** plus 5 mM NB and analyzed by MALDI-TOF mass spectrometry.

of the 25,125 peak (Figure 4C), indicating the inhibitors bind competitively. A small portion of the Hsp90CT was found to be modified by two molecules of **1a**, and therefore an experiment was performed with 10-fold lower concentrations of the photolabile inhibitor (**2**). A significant reduction in the amount of doubly modified Hsp90CT was observed, indicating that the first binding event is most specific (Supplemental Figure 2). To demonstrate cross-linking specificity, apomyoglobin was irradiated in the presence of **1a**, and no cross-linking was observed, confirming selectivity of these compounds for Hsp90 (Figure 4D). Identical cross-linking peaks were detected when **2** was irradiated in the presence of Hsp90, confirming that azide placement on the benzamide side chain did not affect binding.

To determine the peptide sequence to which the photoactivatable derivative was cross-linked, control and **1b**-cross-linked and **2**-cross-linked Hsp90 were digested with trypsin, and the masses of the tryptic peptides were analyzed by ultrahigh mass accuracy Fourier transform ion cyclotron resonance (FTICR) mass spectroscopy (mass accuracy of 10 ppm). Cross-linking of **2** is calculated to increase the theoretical mass of a cross-linked peptide by 527.1613 Da. Analysis of the data identified a peptide corresponding to a mass of ~527 amu greater than that predicted for an unlabeled peptide sequence, namely, 559-KKQEEK-564 or 560-KQEEKK-565 (1316.6093/~MH^{1+} 789.4465 + 527.1540).

As the **2**-linked peptide was present as both a +1 (m/z 1316.60) and +2 (m/z 658.80) ion, MS2 fragmentation of the MH^{2+} 658.80 and MH^{1+} 1316.60 ions was carried out to identity the labeled amino acid (Supplementary Figure 3, Supplementary Scheme 1A, and Supplementary Table 1B). In addition, the fragmentation pattern of NB and the underivatized KKQEEK peptide (m/z 789) were analyzed for comparison to the labeled peptide (Supplementary Figure 4A and B). Consistent with the fragmentation of novobiocin, the MS2 spectrum of the 658.80 and 1316.60 ions contained one dominant ion at 1099.47 corresponding to the loss of noviose and the addition of a proton to maintain the ions positively charged state (Supplementary Figure 3 and Table 1). An ion at 218.12 corresponding to positively charged noviose in the MS2 spectrum of the 658.80 ion reiterated the presence of cross-linked **2** (Supplementary Figure 5 and Supplementary Table 1C). A peak with an m/z of 907 amu was predicted for loss of the aminocoumarin ring; however, this was not observed. In contrast, prominent peaks with m/z of 892.55 (MH^{1+}) and 446.70 (MH^{2+}) were present and are consistent with the loss of the aminocoumarin ring and a CH_3 radical, which occurs upon rearrangement of the aminocycloheptatriene ring to a pyridine ring (Figure 5, Supplementary Scheme 1, Supplementary Figure 3 and Supplementary Table 1B. See Supporting Information and methods for a full detailed discussion of the analysis of the MS data).

Because of the small number of laddering ions observed in the MS2 spectra of the 1312.60 and 658.8 ions, which is common for basic peptides,[28] MS2 peaks were selected and analyzed by MS3 to elucidate the exact peptide sequence. The MS3 spectra of the 1099 peak resulting from the parental 658.80 MH^{2+} (Supplementary Figure 6 and 7 and Supplemental Table 2) and 1316.60 MH^{1+} ions (Supplemental Figure 3 and Supplemental Table 2) confirmed fragmentation of the 1099 (KK-R2QEEK, Figure 5) and 892 (KK-R3QEEK) ions. The presence of y4 and y3 ions minus one or two NH_3 in the fragmentation pattern of the 1099 ion was consistent with a KKQEEK sequence rather than KQEEKK. The MS3 spectra of the 389 ion that was present in the MS2 spectra of the 658.80 MH2+ ion indicated a z3 EEK ion (Figure 5 and Supplemental Table 2), further confirming the peptide sequence.

Together, these results place the photolabile novobiocin derivatives and accordingly, novobiocin, alongside the peptide 559-KKQEEK-564 and attached directly to K560. This segment is located in the Hsp90 C-terminus, within the region of the C-terminal fragment that is protected from proteolysis upon binding to chlorobiocin and novobiocin.

Modeling of NB's Conformation. To further refine the NB binding site in Hsp90, conformations of NB co-crystallized with DNA gyrase/topoisomerase (PDB IDs: 1S14, 1AJ6, 1KIJ) were analyzed. NB was found to adopt a partially folded conformation in each of these structures. This conformation of NB was extracted and used to dock into the site of Hsp90 identified *via* photoaffinity labeling.

Modeling of the Hsp90 NB Binding Site. The data generated from the photoaffinity labeling studies with NB provides information regarding the putative binding site of NB. After careful analysis of the homologous peptide in the full length crystal structure of yeast Hsp90 (538-AEREKEIK-545), it was not clear whether there was a pocket large enough to accommodate NB in the regions flanking this peptide. Initial attempts to dock novobiocin with this crystal structure were unsuccessful. However in 2008, the solution structure of the bacterial Hsp90 homologue, HtpG, was determined by Agard and co-workers using SAXS in concert with molecular modeling.[21] As the full length yeast crystal structure depicts Hsp90 in its closed, clamped conformation, it was postulated that the extended form, as found in solution, would unveil the C-terminal binding site. Generation of this model allowed for identification of the C-terminal inhibitor binding site using the information garnered from the photoaffinity and proteolytic studies.

In an effort to correlate the binding site identified by photoaffinity studies with the open structure of Hsp90α, a homology model of hHsp90α was generated using the SAXS structure of HtpG (dimer) as the template. The homology model of hHsp90α was constructed using software "Modeller".[29] The modeled structure was subsequently subjected to a molecular dynamics protocol for further refinement.

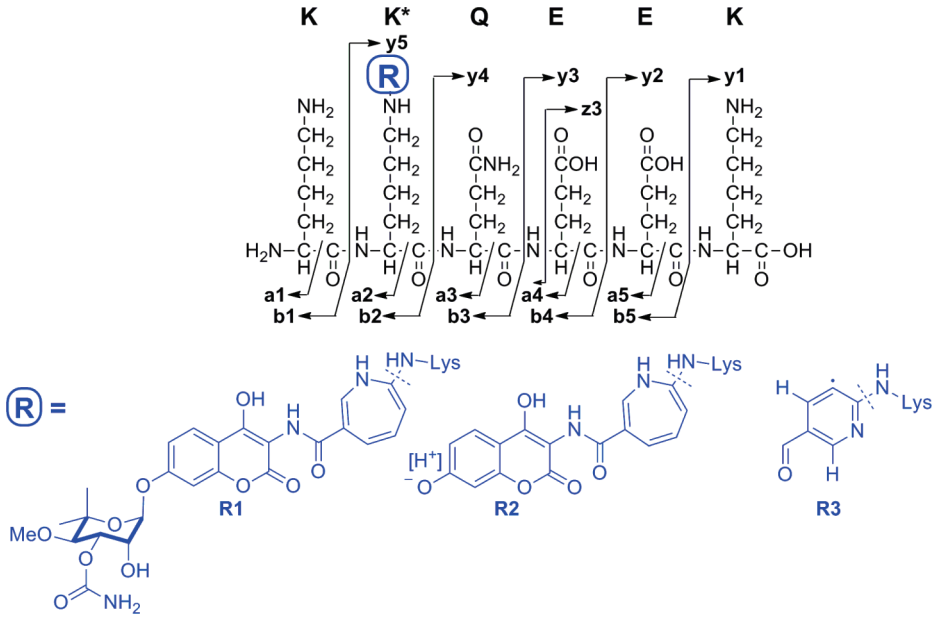

Figure 5. Laddering ions generated from the 2-cross-linked peptides. R1, R2, and R3 represent the major fragmentation products generated from cross-linking with **2**.

Docking of NB into the hHsp90α homology model was guided by the following constraints: (i) binding of NB to the C-terminal domain protects residues in the N-terminal region of the construct from proteolysis by V8 protease, (ii) proteolytic fingerprinting identified the peptide KKQEEK in human Hsp90α as the site of cross-linking for photoreactive NB derivative, and (iii) the bioactive conformation of NB. NB was docked rigidly in the hHsp90α C-terminus by maintaining a distance constraint of 3.5 Å between the hydroxyl of the noviose and the amide nitrogen of Asn686. A multiple sequence alignment of related proteins from different organisms indicated two conserved residues adjacent to the photoaffinity-labeled peptide fragment, Lys538 and Glu562 in hHsp90α. Another residue that is highly conserved is Lys558 in hHsp90α. Minimization of protein side chains with a distance constraint of 3.5 Å between NB and residues Asn686, Lys538, and Glu562 was carried out while keeping NB and the protein backbone rigid to allow relaxation of the side chains and minimization of negative interactions. The binding site was subsequently defined as residues that reside within 8 Å of NB and were subjected to minimization while keeping the rest of the protein and NB fixed to remove unfavorable steric and hydrophobic contacts and to allow side chains to relax and to facilitate NB alignment in the cavity. The resulting complex was further refined by a short MD simulation (100 ps). This Hsp90α−NB complex was found to be stable after simulation. (rmsd <2 Å) The interactions manifested between NB and Hsp90α are depicted in Figure 6.

It is evident from Figure 6B and C that NB is responsible for providing important interactions with several of the residues present in the binding site. These interactions can be summarized as follows: (i) a hydrogen-bonding interaction between the noviose sugar hydroxyl of novobiocin and Asn686 and Thr540 of hHsp90α; (ii) hydrogen-bonding interactions between the oxygen of the prenylated hydroxylphenyl ring of novobiocin and both Asn590 and Lys560 of hHsp90α, a residue identified *via* photoaffinity labeling studies; (iii) the CO and -NH of the noviose carbamate of novobiocin is making hydrogen-bonding interactions with Glu537 and Gln682; (iv) Thr594 provides hydrogen-bonding interactions with the oxygen of the glycosidic bond linking the noviose and coumarin ring; and (v) hydrogen-bonding interaction between the noviose methoxy group and Arg591.

Biochemically guided modeling based on the bacterial homologue of Hsp90, HtpG, produced a human Hsp90 model that upon further refinement unveiled the binding mode for Hsp90 C-terminal inhibitors. This mode of binding explains many of the previously observed biological and biochemical consequences that result upon Hsp90 C-terminal inhibition.

Although there have been previous attempts to model the NB binding site, the results were not consistent with available biochemical data. Prior models developed for the Hsp90 C-terminal inhibitor binding site were generated using homology modeling, MD simulations, and pocket-finder algorithms.[30,31] However, using biochemical analyses, affinity labeling, and homology modeling, we have identified a binding site for C-terminal Hsp90 inhibitors that supports prior biochemical studies.

For example, Neckers and co-workers originally proposed the existence of a binding site in the Hsp90 C-terminus and determined that NB binding was localized to residues 542−732 (hHsp90α).[9,10] It was also demonstrated that addition of the C-terminal peptide 667−680 (hHsp90α) reduced Hsp90's ability to bind immobilized NB, and Hsp90 binding to immobilized NB could be competed with this peptide.[9] In the model proposed, this peptide sequence is located in the α-helix proximal to the sugar binding pocket of NB and is important for interactions with the noviose moiety on NB. Consistent with this pocket being adjacent to the NB binding site, Hartson and co-workers have shown that NB blocks the AC88 antibody (a monoclonal antibody that recognizes an epitope within the amino acids 668−684 in hHsp90α[32]) from binding Hsp90,[12] thus providing two key pieces of previously reported biochemical data that further supports the location of this binding site.

Furthermore, ATP binding plays an important role in the conformational reorganization of Hsp90, in a manner complementary to

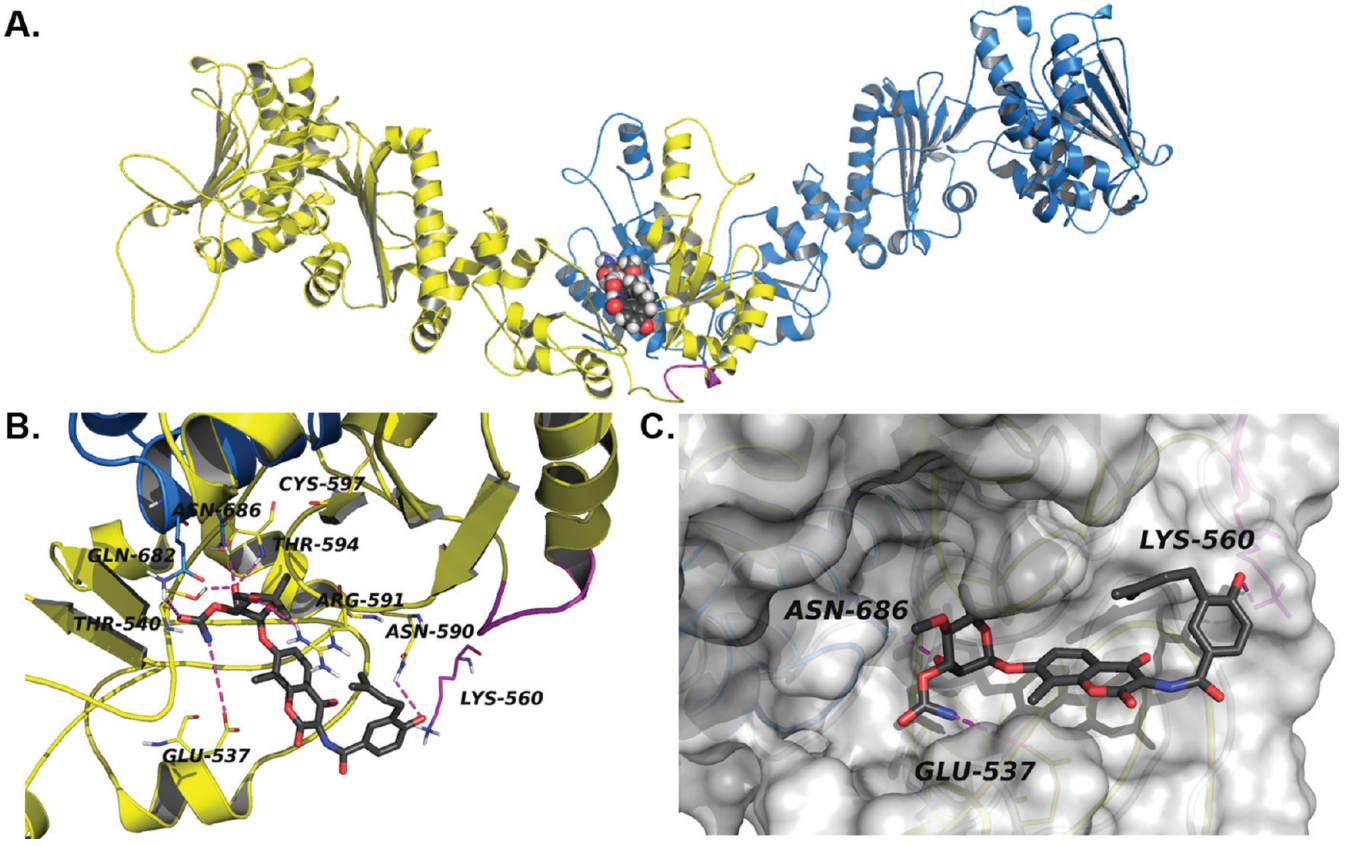

Figure 6. Modeled structure of the Novobiocin binding site in hHsp90α. (A) TheHsp90 α homology model homodimer and the C-terminal binding site with NB (spheres) docked at the interface of two monomers (blue and yellow). (B) Close-up of NB (gray sticks) docked in hHsp90α homology model. The cross-linked fragment and predicted hydrogen bonds (dashes) are depicted in magenta. (C) Surface representation of Hsp90 α homology model CT binding site with NB (gray sticks) docked. Only one molecule of NB is shown to be bound to Hsp90 homodimer; an equivalent binding site contained on the other monomer has not been shown for clarity.

the dimerization of two Hsp90 monomers at the C-terminus, which is essential for Hsp90 activity. Once dimerization occurs at the C-terminus, Hsp90 undergoes a complex conformational cycle that facilitates reorganization and folding of client proteins.[33,34] The C-terminal inhibitor, Coumermycin A1, was shown to disrupt C-terminal dimerization and halt the conformational cycle.[11] In addition, the protein folding process involves a multitude of co-chaperones and partner proteins. Novobiocin and related antibiotics have been shown to disrupt interactions with partner proteins that bind Hsp90 at both the C- and N-terminus, *i.e.*, Cdc37, p23, Hsc70, FKBP52 and PP5.[9,11,12] C-Terminal inhibitors also prevent the binding of small molecules to the N-terminus.[10] Additionally, prior proteolysis experiments and those presented herein with NB and related family members demonstrate that C-terminal occupation protects Hsp90 from proteolysis by altering its conformational state. Specifically, NB shields Lys615 and Arg620 from cleavage. This result can be explained by the examination of Hsp90 in its various conformational states. Lys615 and Arg620 (hHsp90α) are solvent-exposed on the surface of an α helix in the semiclosed and closed states. However, in the extended form, Lys615 and Arg620 are shielded by surrounding residues and hence are not accessible to proteases. Interestingly, the pivot point of Hsp90's movement between the middle and C-terminal domains of Hsp90 (hHsp90α residue 550) is located within close proximity to this binding site.[20,21,23] Taken together, these data indicate that conformational changes within the C-terminus occur upon inhibitor binding and cause global conformational changes within the entire homodimer.

Additionally, Retzlaff and co-workers have demonstrated through mutational analyses that Hsp90 is regulated by a switch point in its C-terminal domain.[35] Mutation of the residue equivalent to Cys597 in hHsp90α (Ile538 in HtpG) altered Hsp90's ATPase and chaperone activity, modified N-terminal and C-terminal domain associations, and shifted the conformational equilibrium of Hsp90 within its ATPase cycle.[35] In our model, Cys597 forms part of the NB binding pocket (Figure 6B). Thus, the model suggests that C-terminal inhibitors have the ability to interact with and stabilize the region around this pivot point and prohibit the global conformational changes required for chaperone activity. Consequently, upon C-terminal occupation, the Hsp90 machinery is stalled in the open conformation, which results in protection of Lys615 and Arg620 from proteolysis, hinders N-terminal ATP hydrolysis, and prevents the binding of N-terminal inhibitors. Once again, occupation of this putative binding pocket in the Hsp90 C-terminus can finally explain previously observed biochemical observations.

In addition, Hugel and co-workers recently determined the dynamics and kinetics of C-terminal dimerization, whereby the C-terminus is capable of opening in the presence of N-terminal ligands (*i.e.*, ATP and ATP analogues). Additionally, it was observed that N- and C-terminal dimerization is intimately related and

that C-terminal dimerization is not required for N-terminal dimerization. These findings suggest that the C-terminus is in constant flux, whereby a multitude of conformations exist.[24] In the model presented herein, novobiocin predominantly interacts with one monomer of the Hsp90 homodimer. Together with the data presented by Hugel, it can be reasoned that small molecule binding to the Hsp90 C-terminus may occur while this domain is open, preventing dimerization and continuation through the catalytic cycle. Alternatively, C-terminal inhibitors may bind after dimerization, preventing occupation of the N-terminal binding pocket by ATP, which is supported by prior studies by Marcu *et al.*, who demonstrated that novobiocin binding to the C-terminus prevented N-terminal occupation.[10]

Hsp90 C-terminal inhibitors have garnered significant attention during the past decade, specifically due to problems associated with N-terminal inhibition in the clinic.[36] Structural information regarding the C-terminus, especially the NB binding site, has been scarce, and attempts at co-crystallization have been unsuccessful. Accordingly, effective analogue design and data analysis has been hindered. Therefore, we have utilized photoaffinity labeling and proteolytic studies to identify residues that form the NB binding site. Through elucidation of the cross-linked peptide and molecular modeling alongside the reported solution structure of Hsp90, potential binding sites were carefully evaluated. As a result of these studies and those before us, we are finally able to provide a binding site for NB and other C-terminal inhibitors that accounts for the biological activities manifested by NB. This model provides a new paradigm for the development of future Hsp90 inhibitors that target the C-terminal binding pocket.

METHODS

Characterization of the Protease-Resistant Core of Hsp90CT. Recombinant His-tagged Hsp90CT (amino acids 531−732 human Hsp90α) was incubated with V8 protease at 37 °C in the presence of 800 μM Chlorobiocin or an equivalent volume of DMSO (vehicle control). Protease resistant bands were separated by SDS-PAGE, excised, digested with trypsin, and analyzed by LC−MS/MS as described in the Supporting Information.

Identification of the NB Binding Site in Hsp90CT. After optimization of cross-linking conditions with **1** (Figure 3), recombinant His-tagged Hsp90CT was exposed to four flashes of 184 μJ of UV radiation in the presence of 0.5 mM of either **1**, **2**, or DMSO (vehicle control), followed by digestion of the samples with trypsin. The tryptic peptides were subjected to capillary LC−MS/MS experiments using a tandem LTQ-FT Mass Spectrometer (ThermoFinnigan) under conditions described previously,[37] followed by data analysis as described in the Supporting Information.

Refinement of Hsp90α Structure. The sequence of hHsp90α was used to search similar sequences using NCBI blast.[38] A multiple sequence alignment was performed using ClustalW with default parameters to align these sequences and to identify structurally conserved regions and important residues.[39] The minimization of the side chains was performed using Sybyl molecular modeling software.[40] Initially, the protein was held fixed except for the binding site residues (residues falling within 8 Å of novobiocin molecule). Thereafter, all side chains and the binding site were kept free and minimization was done. All the minimization was done until the rms gradient of 0.05 kcal/mol Å was obtained using AMBER9 force field.

Molecular Dynamics Protocol. Hsp90α-NB was prepared for simulation in AMBER9 package while the simulation was done using NAMD software.[41] The force field parameters for NB were calculated by antechamber module of AMBER9. The HtpG-NB complex was solvated in a box of water with buffering distance of 10 Å; assuming normal charge states of ionizable groups corresponding to pH 7, sodium (Na^+) and chloride (Cl^-) counterions were added to achieve charge neutrality and to mimic biological environment more closely. All Na^+ and Cl^- ions were placed at least 8 Å away from any protein atoms and from each other. The system was subjected to initial minimization for 20,000 steps (40 ps) keeping the protein backbone fixed, which was followed by 20,000 steps (40 ps) of minimization without fixing anything (to allow system to relax freely). Further details of the molecular dynamics protocol used to compute the final model and homology modeling of the NB binding site in Hsp90α are presented in Supporting Information.

ASSOCIATED CONTENT

Supporting Information. This material is available free of charge *via* the Internet at http://pubs.acs.org.

AUTHOR INFORMATION

Corresponding Author

*Tel: +1 785-864-2288. Fax: +1 785-864-5326. E-mail: bblagg@ku.edu.

ACKNOWLEDGMENT

The authors gratefully acknowledge the support of this project by NIH CA120458 (B.S.J.B.), the Oklahoma Agricultural Experiment Station (Project No. 1975), NIH CA125392 (R.L.M.), NIH Training Grant (T32 GM008545) on Dynamic Aspects in Chemical Biology (L.B.P.), ACS Division of Medicinal Chemistry Predoctoral Fellowship (L.B.P.), the Concern Foundation (CF0406, S.D.H.), and NSF MRI and EPSCoR programs (award 0722494, S.D.H.). We would also like to thank D. Agard for the coordinates of the open HtpG SAXS structure.

REFERENCES

(1) Pearl, L. H., and Prodromou, C. (2006) Structure and mechanism of the Hsp90 molecular chaperone machinery. *Annu. Rev. Biochem. 75*, 271–294.

(2) Pearl, L. H., Prodromou, C., and Workman, P. (2008) The Hsp90 molecular chaperone: an open and shut case for treatment. *Biochem. J. 410*, 439–453.

(3) Hanahan, D., and Weinberg, R. A. (2000) The hallmarks of cancer. *Cell 100*, 57–70.

(4) Bishop, S. C., Burlison, J. A., and Blagg, B. S. J. (2007) Hsp90: a novel target for the disruption of multiple signaling cascades. *Curr. Cancer Drug Targets 7*, 369–388.

(5) McDonald, E., Workman, P., and Jones, K. (2006) Inhibitors of the Hsp90 molecular chaperone: attacking the master regulator in cancer. *Curr. Top. Med. Chem. 6*, 1091–1107.

(6) Roe, S. M., Prodromou, C., O'Brien, R., Ladbury, J. E., Piper, P. W., and Pearl, L. H. (1999) Structural basis for inhibition of the Hsp90 molecular chaperone by the antitumor antibiotics radicicol and geldanamycin. *J. Med. Chem. 42*, 260–266.

(7) Stebbins, C. E., Russo, A. A., Schneider, C., Rosen, N., Hartl, F. U., and Pavletich, N. P. (1997) Crystal structure of an Hsp90-geldanamycin complex: Targeting of a protein chaperone by an antitumor agent. *Cell 89*, 239–250.

(8) Biamonte, M. A., Van de Water, R., Arndt, J. W., Scannevin, R. H., Perret, D., and Lee, W. (2010) Heat shock protein 90: inhibitors in clinical trials. *J. Med. Chem. 53*, 3–17.

(9) Marcu, M. G., Chadli, A., Bouhouche, I., Catelli, M., and Neckers, L. M. (2000) The heat shock protein 90 antagonist novobiocin interacts with a previously unrecognized ATP-binding domain in the carboxyl terminus of the chaperone. *J. Biol. Chem. 275*, 37181–37186.

(10) Marcu, M. G., Schulte, T. W., and Neckers, L. (2000) Novobiocin and related coumarins and depletion of heat shock protein 90-dependent signaling proteins. *J. Natl. Cancer Inst. 92*, 242–248.
(11) Allan, R. K., Mok, D., Ward, B. K., and Ratajczak, T. (2006) Modulation of chaperone function and cochaperone interaction by novobiocin in the C-terminal domain of Hsp90: evidence that coumarin antibiotics disrupt Hsp90 dimerization. *J. Biol. Chem. 281*, 7161–7171.
(12) Yun, B.-G., Huang, W., Leach, N., Hartson, S. D., and Matts, R. L. (2004) Novobiocin induces a distinct conformation of Hsp90 and alters Hsp90-cochaperone-client interactions. *Biochemistry 43*, 8217–8229.
(13) Galam, L., Hadden, M. K., Ma, Z., Ye, Q. Z., Yun, B. G., Blagg, B. S., and Matts, R. L. (2007) High-throughput assay for the identification of Hsp90 inhibitors based on Hsp90-dependent refolding of firefly luciferase. *Bioorg. Med. Chem. 15*, 1939–1946.
(14) Burlison, J. A., Avila, C., Vielhauer, G., Lubbers, D. J., Holzbeierlein, J., and Blagg, B. S. (2008) Development of novobiocin analogues that manifest anti-proliferative activity against several cancer cell lines. *J. Org. Chem. 73*, 2130–2137.
(15) Burlison, J. A., and Blagg, B. S. (2006) Synthesis and evaluation of coumermycin A1 analogues that inhibit the Hsp90 protein folding machinery. *Org. Lett. 8*, 4855–4858.
(16) Donnelly, A., and Blagg, B. S. (2008) Novobiocin and additional inhibitors of the Hsp90 C-terminal nucleotide-binding pocket. *Curr. Med. Chem. 15*, 2702–2717.
(17) Matthews, S. B., Vielhauer, G. A., Manthe, C. A., Chaguturu, V. K., Szabla, K., Matts, R. L., Donnelly, A. C., Blagg, B. S., and Holzbeierlein, J. M. (2010) Characterization of a novel novobiocin analogue as a putative C-terminal inhibitor of heat shock protein 90 in prostate cancer cells. *Prostate 70*, 27–36.
(18) Shelton, S. N., Shawgo, M. E., Matthews, S. B., Lu, Y., Donnelly, A. C., Szabla, K., Tanol, M., Vielhauer, G. A., Rajewski, R. A., Matts, R. L., Blagg, B. S., and Robertson, J. D. (2009) KU135, a novel novobiocin-derived C-terminal inhibitor of the 90-kDa heat shock protein, exerts potent antiproliferative effects in human leukemic cells. *Mol. Pharmacol. 76*, 1314–1322.
(19) Yu, X. M., Shen, G., Neckers, L., Blake, H., Holzbeierlein, J., Cronk, B., and Blagg, B. S. (2005) Hsp90 inhibitors identified from a library of novobiocin analogues. *J. Am. Chem. Soc. 127*, 12778–12779.
(20) Krukenberg, K. A., Bottcher, U. M., Southworth, D. R., and Agard, D. A. (2009) Grp94, the endoplasmic reticulum Hsp90, has a similar solution conformation to cytosolic Hsp90 in the absence of nucleotide. *Protein Sci. 18*, 1815–1827.
(21) Krukenberg, K. A., Forster, F., Rice, L. M., Sali, A., and Agard, D. A. (2008) Multiple conformations of *E. coli* Hsp90 in solution: insights into the conformational dynamics of Hsp90. *Structure 16*, 755–765.
(22) Bron, P., Giudice, E., Rolland, J. P., Buey, R. M., Barbier, P., Diaz, J. F., Peyrot, V., Thomas, D., and Garnier, C. (2008) Apo-Hsp90 coexists in two open conformational states in solution. *Biol. Cell 100*, 413–425.
(23) Southworth, D. R., and Agard, D. A. (2008) Species-dependent ensembles of conserved conformational states define the Hsp90 chaperone ATPase cycle. *Mol. Cell 32*, 631–640.
(24) Ratzke, C., Mickler, M., Hellenkamp, B., Buchner, J., and Hugel, T. (2010) Dynamics of heat shock protein 90 C-terminal dimerization is an important part of its conformational cycle. *Proc. Natl. Acad. Sci. U.S.A. 107*, 16101–16106.
(25) Bellon, S., Parsons, J. D., Wei, Y., Hayakawa, K., Swenson, L. L., Charifson, P. S., Lippke, J. A., Aldape, R., and Gross, C. H. (2004) Crystal structures of *Escherichia coli* topoisomerase IV ParE subunit (24 and 43 kDas): a single residue dictates differences in novobiocin potency against topoisomerase IV and DNA gyrase. *Antimicrob. Agents Chemother. 48*, 1856–1864.
(26) Holdgate, G. A., Tunnicliffe, A., Ward, W. H., Weston, S. A., Rosenbrock, G., Barth, P. T., Taylor, I. W., Pauptit, R. A., and Timms, D. (1997) The entropic penalty of ordered water accounts for weaker binding of the antibiotic novobiocin to a resistant mutant of DNA gyrase: a thermodynamic and crystallographic study. *Biochemistry 36*, 9663–9673.
(27) Shen, G., Yu, X. m., and Blagg, B. S. J. (2004) Syntheses of photolabile novobiocin analogues. *Bioorg. Med. Chem. Lett. 14*, 5903–5906.
(28) Tang, X. J., Thibault, P., and Boyd, R. K. (1993) Fragmentation reactions of multiply-protonated peptides and implications for sequencing by tandem mass spectrometry with low-energy collision-induced dissociation. *Anal. Chem. 65*, 2824–2834.
(29) Sali, A., and Blundell, T. L. (1993) Comparative protein modelling by satisfaction of spatial restraints. *J. Mol. Biol. 234*, 779–815.
(30) Sgobba, M., Degliesposti, G., Ferrari, A. M., and Rastelli, G. (2008) Structural models and binding site prediction of the C-terminal domain of human Hsp90: a new target for anticancer drugs. *Chem. Biol. Drug Des. 71*, 420–433.
(31) Sgobba, M., Forestiero, R., Degliesposti, G., and Rastelli, G. (2010) Exploring the binding site of C-terminal Hsp90 inhibitors. *J. Chem. Inf. Comp. Sci. 50*, 1522–1528.
(32) Hartson, S. D., Thulasiraman, V., Huang, W., Whitesell, L., and Matts, R. L. (1999) Molybdate inhibits Hsp90, induces structural changes in its C-terminal domain, and alters its interactions with substrates. *Biochemistry 38*, 3837–3849.
(33) Ali, M. M., Roe, S. M., Vaughan, C. K., Meyer, P., Panaretou, B., Piper, P. W., Prodromou, C., and Pearl, L. H. (2006) Crystal structure of an Hsp90-nucleotide-p23/Sba1 closed chaperone complex. *Nature 440*, 1013–1017.
(34) Richter, K., Soroka, J., Skalniak, L., Leskovar, A., Hessling, M., Reinstein, J., and Buchner, J. (2008) Conserved conformational changes in the ATPase cycle of human Hsp90. *J. Biol. Chem. 283*, 17757–17765.
(35) Retzlaff, M., Stahl, M., Eberl, H. C., Lagleder, S., Beck, J., Kessler, H., and Buchner, J. (2009) Hsp90 is regulated by a switch point in the C-terminal domain. *EMBO Rep. 10*, 1147–1153.
(36) Duerfeldt, A. S., and Blagg, B. S. J. (2010) Hsp90 inhibition: Elimination of shock and stress. *Bioorg. Med. Chem. Lett. 20*, 4983–4987.
(37) Ikehata, K., Duzhak, T. G., Galeva, N. A., Ji, T., Koen, Y. M., and Hanzlik, R. P. (2008) Protein targets of reactive metabolites of thiobenzamide in rat liver in vivo. *Chem. Res. Toxicol. 21*, 1432–1442.
(38) Altschul, S. F., Gish, W., Miller, W., Myers, E. W., and Lipman, D. J. (1990) Basic local alignment search tool. *J. Mol. Biol. 215*, 403–410.
(39) Larkin, M. A., Blackshields, G., Brown, N. P., Chenna, R., McGettigan, P. A., McWilliam, H., Valentin, F., Wallace, I. M., Wilm, A., Lopez, R., Thompson, J. D., Gibson, T. J., and Higgins, D. G. (2007) Clustal W and Clustal X version 2.0. *Bioinformatics 23*, 2947–2948.
(40) *SYBYL*, p 7.3, Tripos International, 1699 South Hanley Rd., St. Louis, Missouri, 63144, USA.
(41) Phillips, J. C., Braun, R., Wang, W., Gumbart, J., Tajkhorshid, E., Villa, E., Chipot, C., Skeel, R. D., Kalé, L., and Schulten, K. (2005) Scalable molecular dynamics with NAMD. *J. Comput. Chem. 26*, 1781–1802.